Absolute electromagnetic transition rates in semi-magic N = 50 isotones as a test for $(\pi g_{9/2})^n$ single particle calculations.

Jan Jolie [1], Mario Ley [1], Andrey Blazhev [1], Arwin Esmaylzadeh [1], Lukas Knafla [1], Aaron Pfeil [1], Christoph Fransen [1], Jean-Marc Regis [1], and Piet Van Isacker [2],

1: IKP, Universität zu Köln, Zülpicher Str. 77, D-50937 Köln, Germany

2: GANIL, CEA/DRF–CNRS/IN2P3, Bvd Henri Becquerel, F-14076 Caen, France

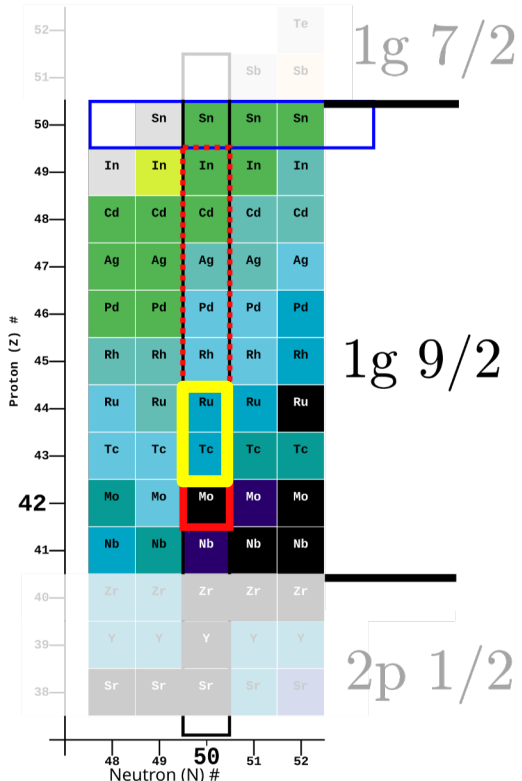

1. Motivation
2. Fast timing using centroid difference methods
3. Experiments on ^{92}Mo and other N = 50 isotones
4. Conclusions

1. Motivation

Untruncated **numerical full shell model calculations** with the SR88MHJM interaction and all proton orbits between Z= 38 and Z=50.

Analytical single-j calculations with a seniority conserving interaction or with empirical two-body matrix elements. Example: ^{93}Tc as $(\pi 1g_{9/2})^3$

$$E(j^3[I]J) = 3\sum_R [j^2(R)jJ|\}j^3[I]J]^2 E(j^2R)$$

Energy of state in ^{93}Tc

Sum over states in ^{92}Mo

CFP^2

Energy of state in ^{92}Mo

A de Shalit and I. Talmi, The Nuclear Shell Model (1963)

Recently, this approach was extended to electromagnetic quadrupole transition rates by Piet Van Isacker.

Assumptions:
Seniority is conserved.
The effective charges in one-body E2 operator of the two-j nucleus can be state dependent.
The effective charges in the quadrupole moment of the state with spin R are the same as those for $B(E2;R \rightarrow R-2) = B_R$ in the two-particle nucleus.

Then the following relation can be obtained:

$$B(\mathrm{E2}; j^3[I]J \rightarrow j^3[I']J') = \left(\sum_R g_j(J, I, J', I', R) \sqrt{B_R} \right)^2$$

First application to ^{135}I as $(\pi 1g_{7/2})^3$ P. Spagnoletti et al. Phys. Rev. C 95 (2017) 021302
Very succesful for ^{211}At using ^{210}Po V. Karayonchev et al., Phys. Rev. C 106, (2022) 044321

2. Fast timing using Centroid Difference Methods

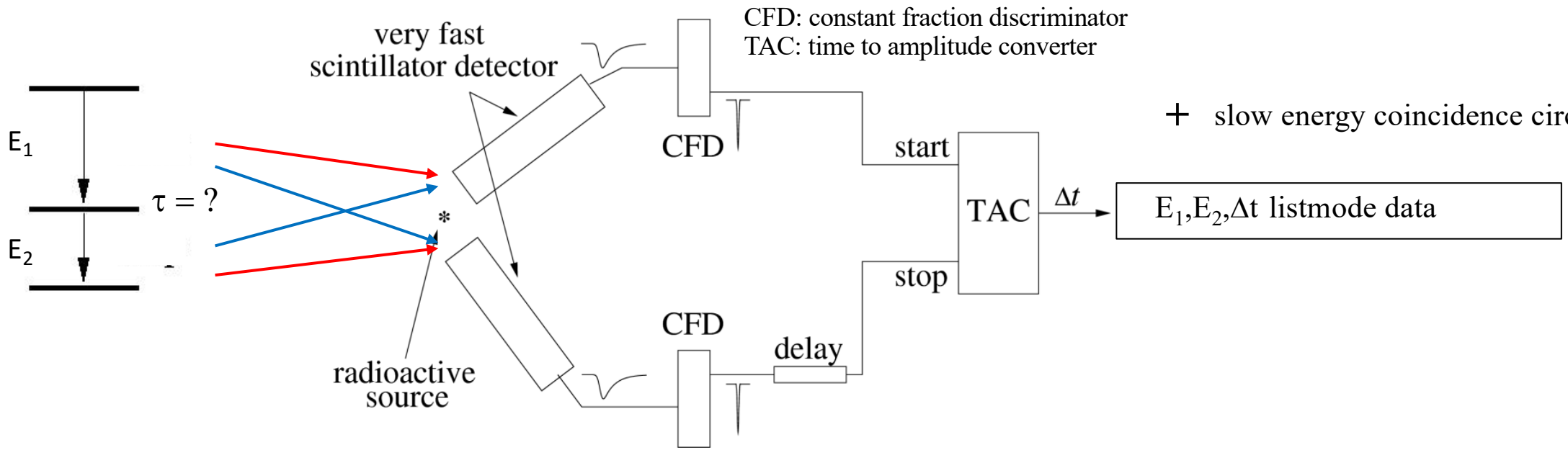

Mirror Symmetric Centroid Difference (MSCD) method

J.M. Régis, G Pascovici, M. Rudigier, J. Jolie NIM A 622 (2010) 83

$$\Delta C_{decay}(\Delta E)=C(D)_{stop}-C(D)_{start}=$$
$$C(P)_{stop}+\tau-(C(P)_{start}-\tau)=PRD(\Delta E)+2\tau$$

Prompt Response Difference (PRD):

$$PRD(\Delta E)= C(P)_{stop}-C(P)_{start}$$
$$PRD(\Delta E) = PRD(E_{feeder}) - PRD(E_{decay})$$

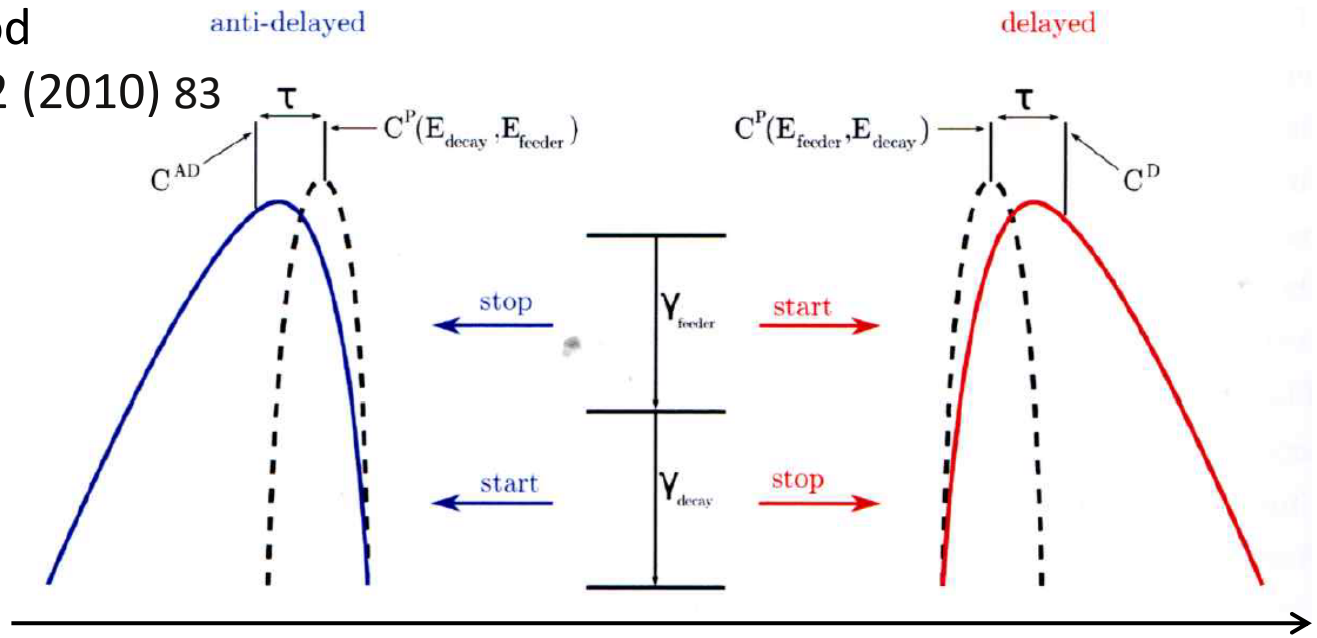

Calibration of the PRD curve using the ^{152}Eu source

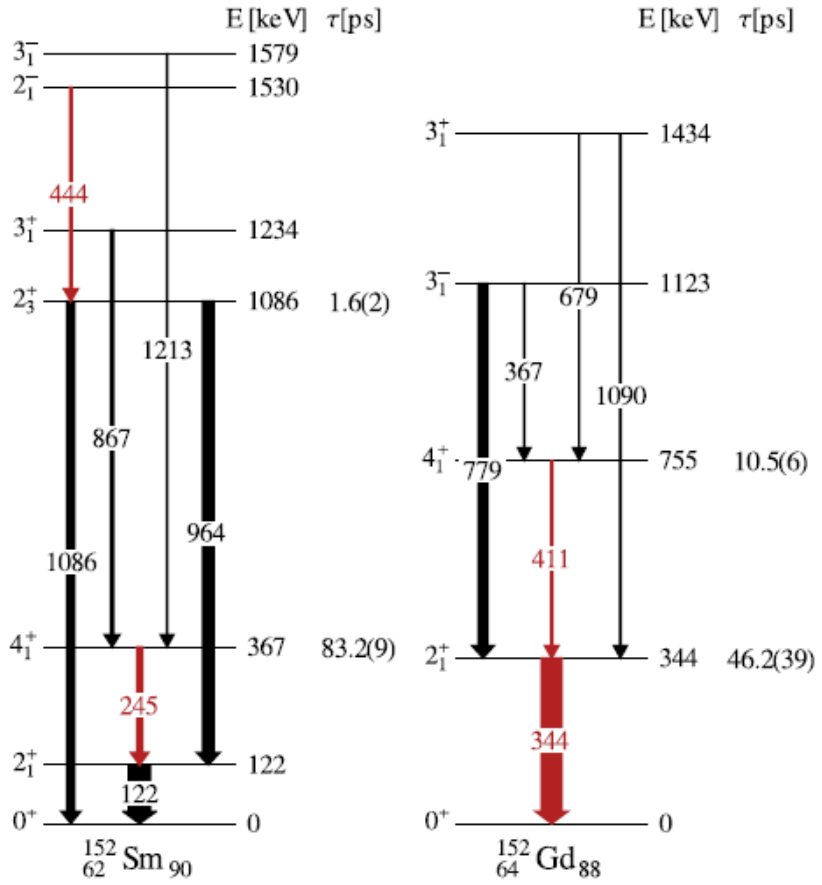

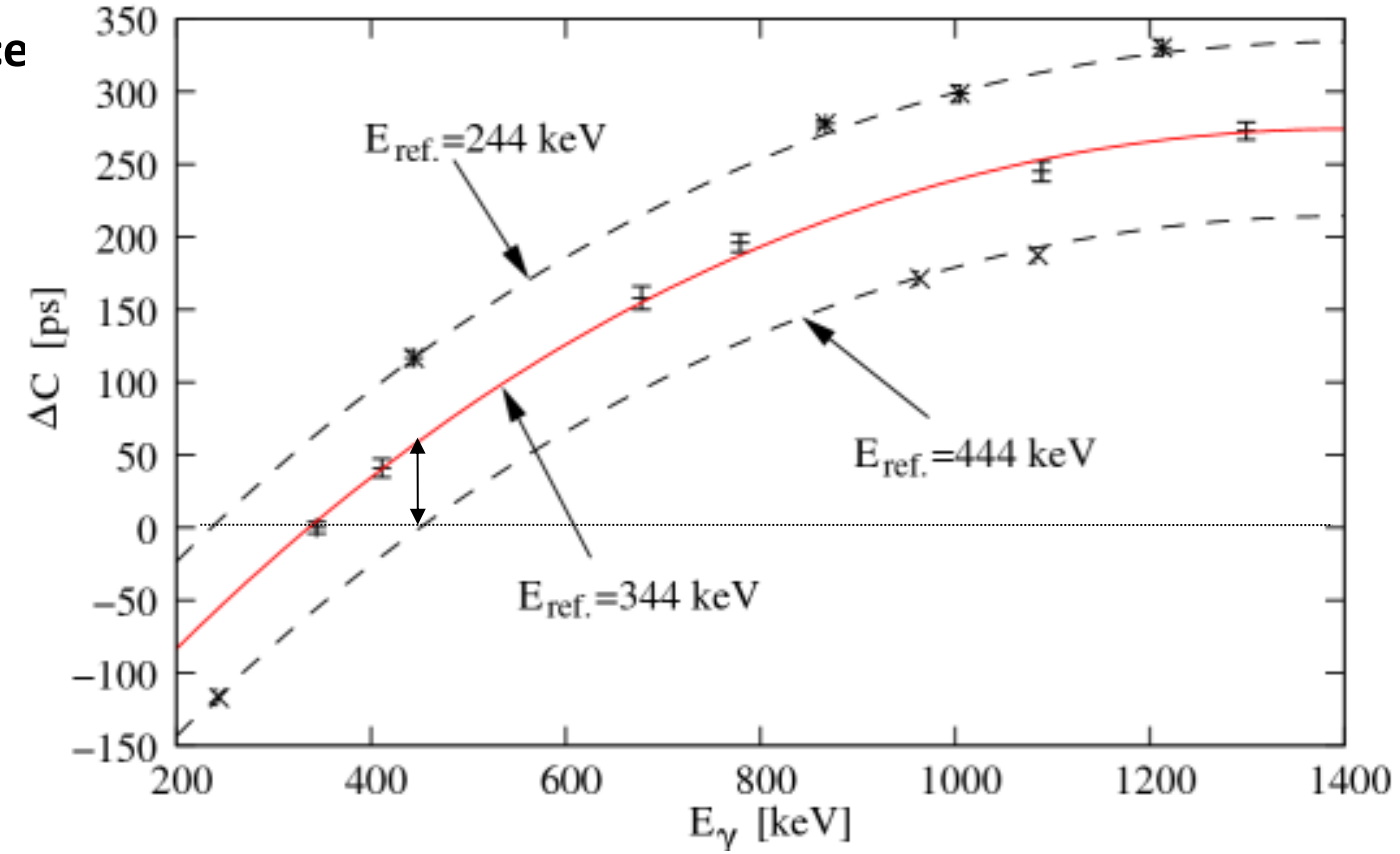

PRD=ΔC-2τ

The PRD curve is shifted in parallel using different reference energies.

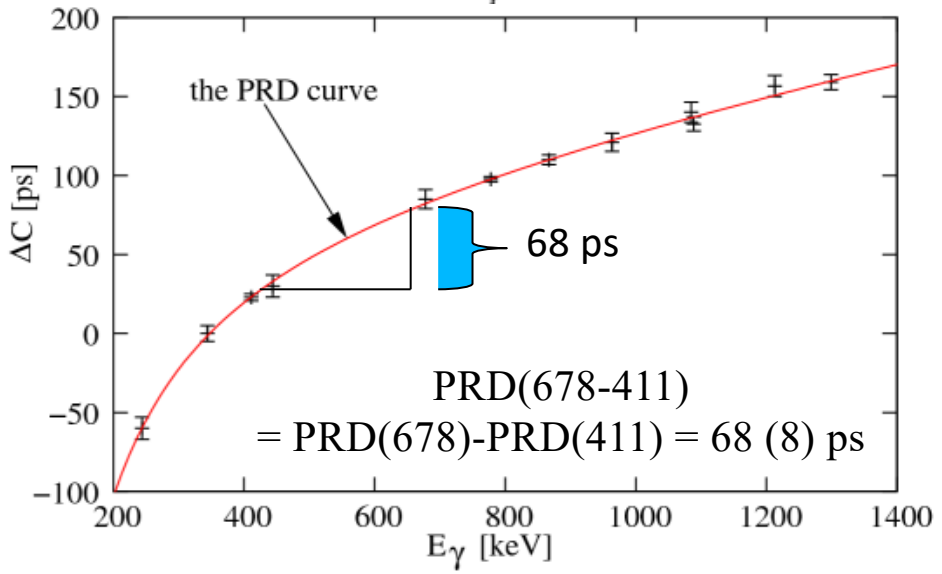

PRD(678-411)
= PRD(678)-PRD(411) = 68 (8) ps

Remeasurement of PRD relevant lifetime of first 2^+ state in ^{152}Gd (4 weeks measurement):
New τ = 46.9(3) ps Old: τ = 46.2(39)
L. Knafla et al. NIM A 1052 (2023), 168279.

The Compton background has an important time dependence which needs to be corrected for.

Example time response using ^{60}Co.

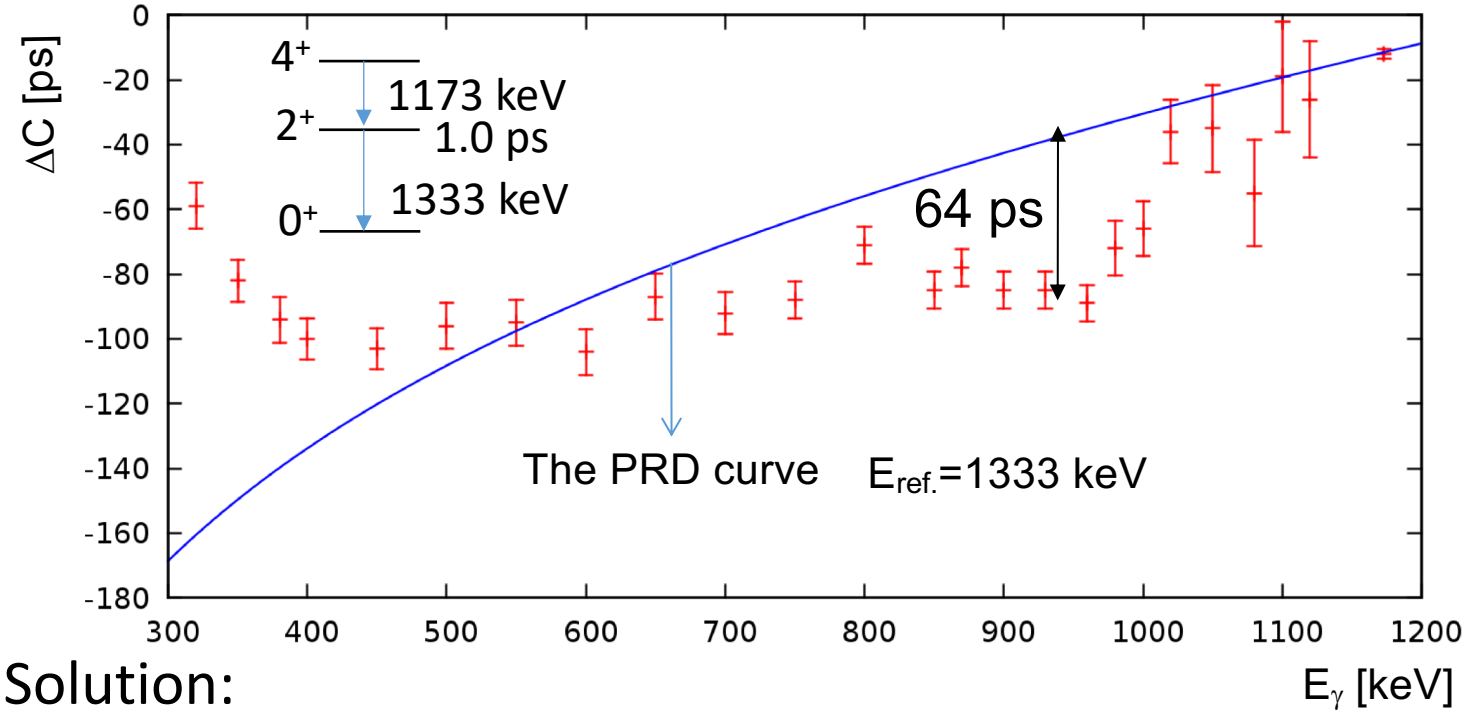

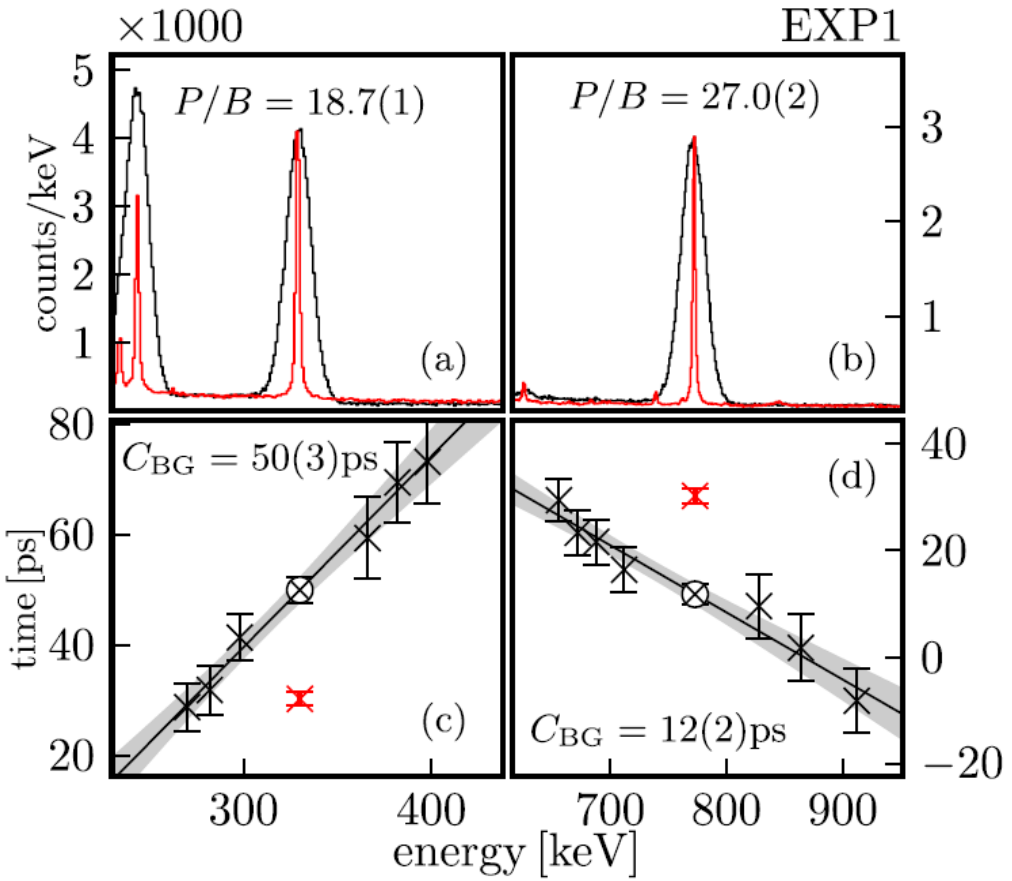

Solution:

Interpolation of background below the used peaks.

$$C_{\mathrm{PP}} = C_{\mathrm{exp}} + \tilde{t}_{\mathrm{cor}},$$

$$\tilde{t}_{\mathrm{cor}} = \frac{P/B(E_f)\,t_{\mathrm{cor}}(E_i) + P/B(E_i)\,t_{\mathrm{cor}}(E_f)}{P/B(E_i) + P/B(E_f)},$$

$$t_{\mathrm{cor}} = \frac{C_{\mathrm{exp}} - C_{\mathrm{BG}}(E)}{P/B(E)},$$

See also H. Mach et al. Nucl. Phys. A 523 (1991) 197 section 2.3.

The Generalized Centroid Difference (GCD) method for γ-γ fast timing arrays

[J.M. Régis et al., NIM A 726 (2013) 191]

The generalisation of the MSCD method was done for the FATIMA@EXILL Array in Spring 2013. It holds for arrays holding the same type of scintillators, all at the same distance from the target. Then the averaged spectra still follow the MSCD relations.

$$\Delta\overline{C}_{decay}\,(\Delta E) = \overline{C}_{stop} - \overline{C}_{start} =$$

$$\overline{PRD}(E_{feeder}) - \overline{PRD}(E_{decay}) + 2\tau$$

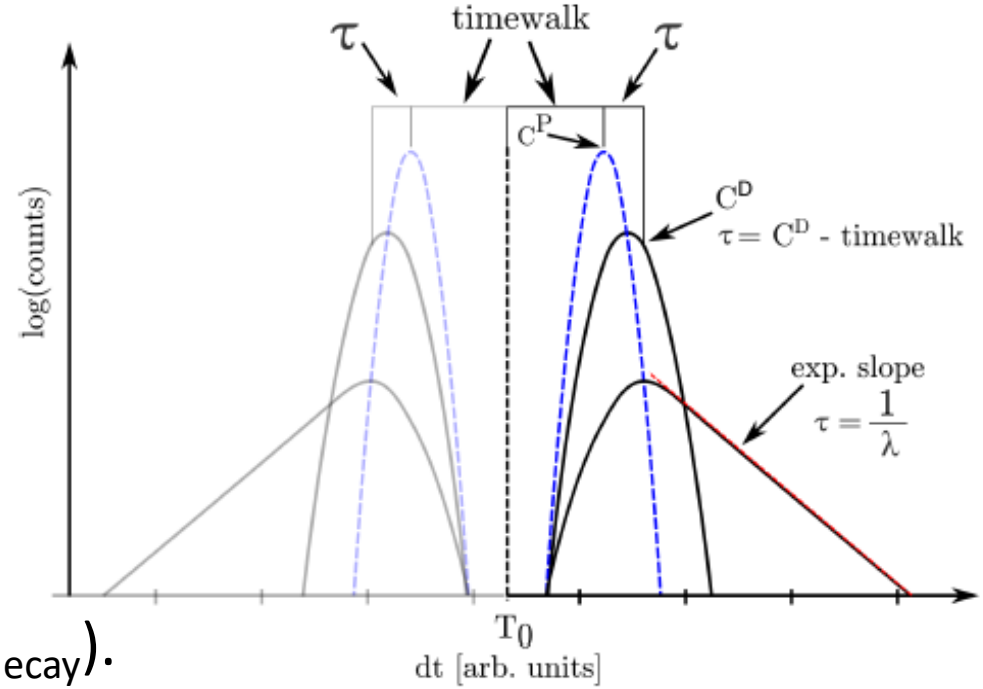

The Symmetrized GCD method:

[J.M. Régis, M. Dannhoff, J. Jolie NIM A 897 (2018) 38]

Using the mirror symmetry between delayed and antidelayed time spectra, the latter can be mirrored and added to the first leading when T_0 is put to zero to: $\tau = C^D - TW\,(E_{feeder}, E_{decay})$.

3. Experiments on ^{92}Mo and other N = 50 isotones.

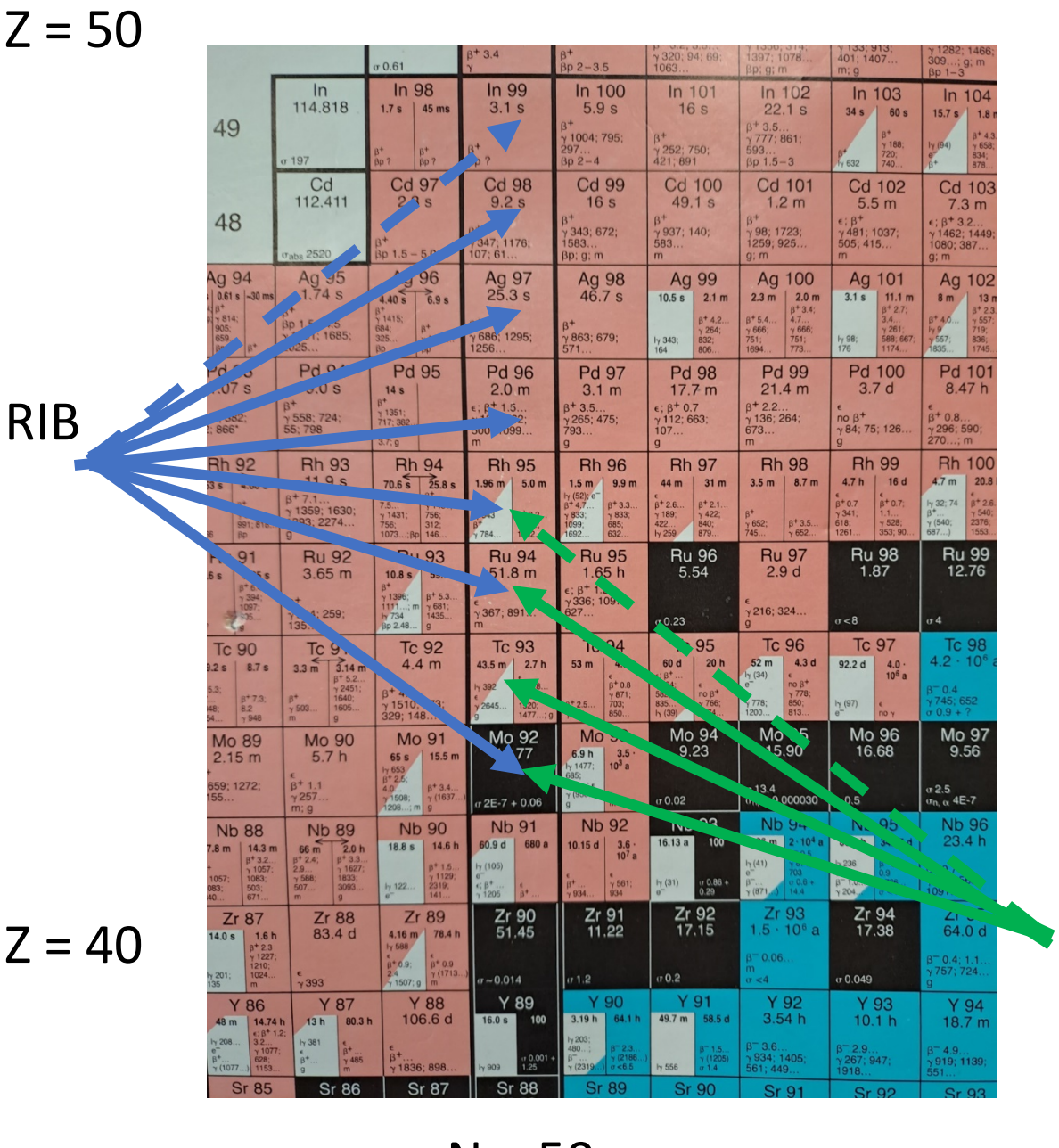

After the success in the N = 126 isotones, it would be interesting to study similar isotones.

Candidates could be the N= 50 isotones above Z= 40 where the $\pi(1g_{9/2})$ orbit gets filled. Also here, the knowledge on lifetimes and B(E2) values is limited and often contradictory or unprecise.

The problem is to populate the isotones above ^{90}Zr using stable or radioactive ion beams.

Here we report on the stable beam experiments performed recently in Cologne.

^{92}Mo:

The main problem is the lifetime of the first 4^+ state which is needed for the prediction of all other B(E2) values. Note B(E2) to first 2^+ known via Coulex.

Recently, the lifetime of the 2^+ and 4^+ states were measured for the first time as 0.8(4) ps and 35.5(6) in a recoil distance experiment at GANIL.
R. M. Pérez-Vidal et al. Phys. Rev. Lett. 129 (2022) 112501.

To verify the lifetime of the first 4^+ state and reduce the statistical and systematic error two fusion evaporation reactions were used at the 10MV Tandem accelerator in Cologne.

EXP1: ^{90}Zr(α,2n)^{92}Mo @ 27 MeV on a 5.3mg cm^{-2} 97.62% enriched target.

EXP2: ^{93}Nb(p,2n)^{92}Mo @ 18 MeV on a 5.4mg cm^{-2} monoisotopic target.

New:
Completely digital acquisition system (CAEN 500MHz digitisers) with digital CFD algorithm to reach timestamps with ps resolution. *A. Harter et al. NIM A 1053 (2023) 168279.*
Symmetrized Analysis. *J. M. Régis et al. NIM A 897 (2018) 3.*
Remeasurement of PRD relevant lifetime in ^{152}Gd. *L. Knafla et al. NIM A 1052 (2023), 168279.*

The HORUS array was equipped with 8 Ge detectors and 9 LaBr3(Ce) scintillators of which 6 with BGO shields.

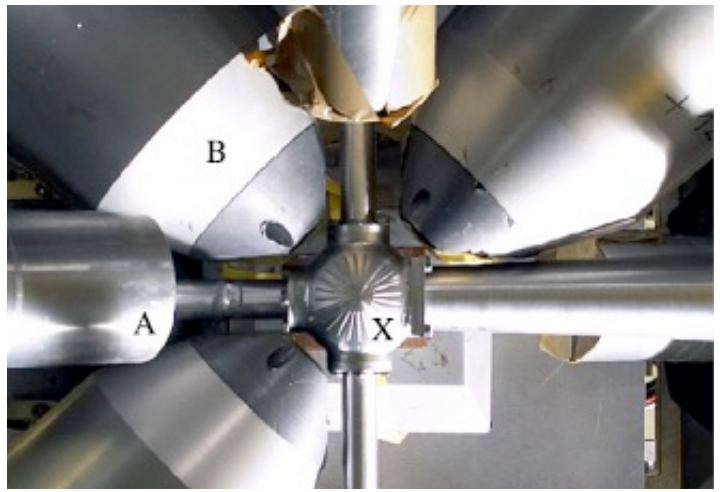

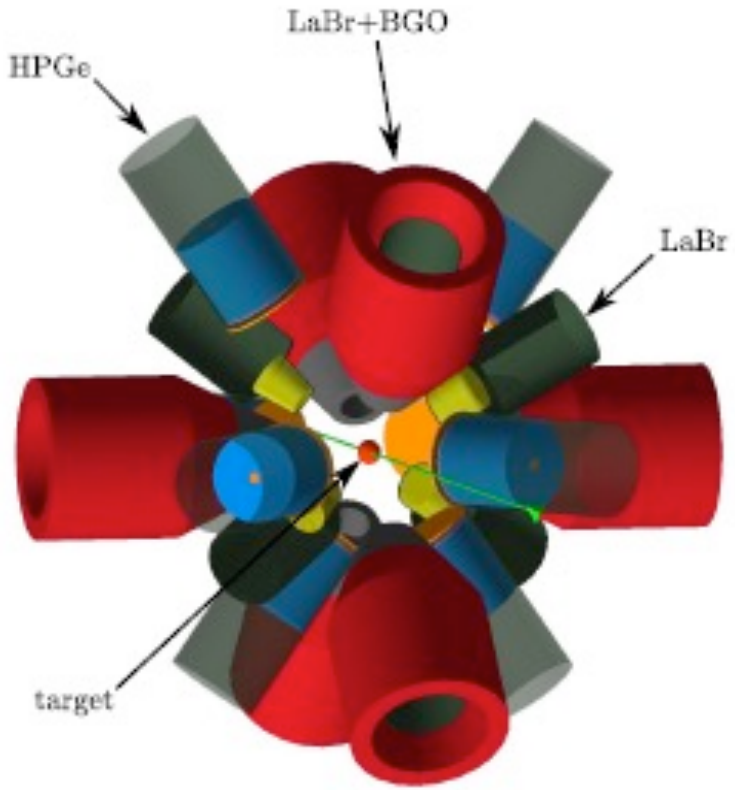

Time Walk (TW) is obtained from a ^{152}Eu source using the new value for the first excited 2^+ state in ^{152}Gd.

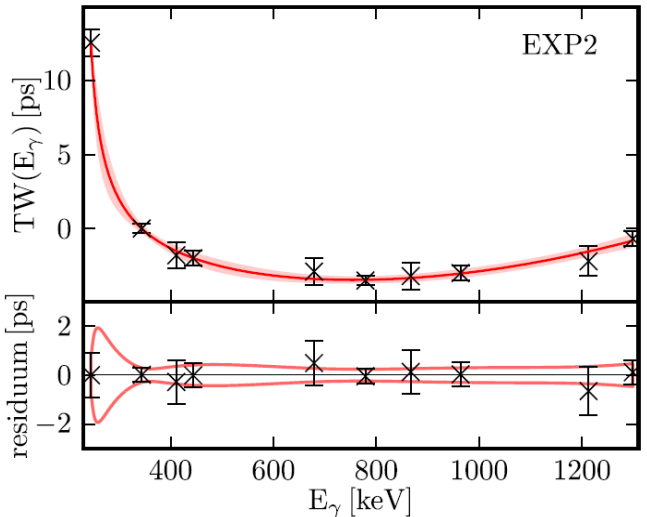

$$C = \tau + TW(E_{\text{feeder}}, E_{\text{decay}}),$$

$$TW(E_{\text{feeder}}, E_{\text{decay}}) = TW(E_{\text{feeder}}) - TW(E_{\text{decay}}).$$

$$TW(E_\gamma) = \frac{a}{\sqrt{E_\gamma + b}} + E_\gamma^2\, c + E_\gamma\, d + e.$$

L. Knafla et al. NIM A 1052 (2023), 168279.

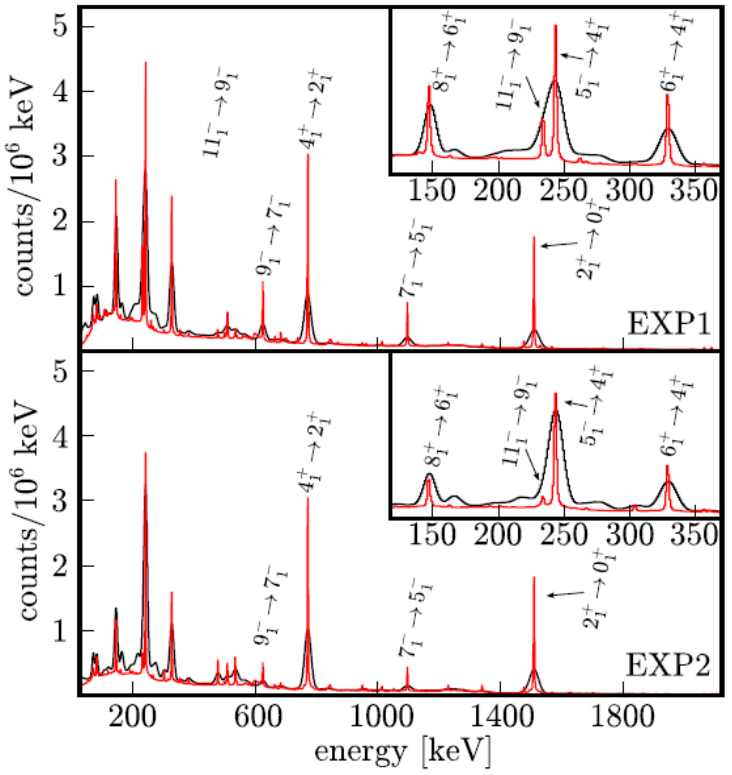

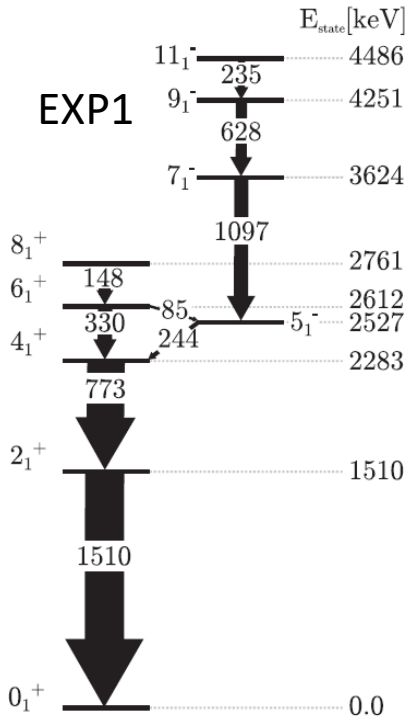

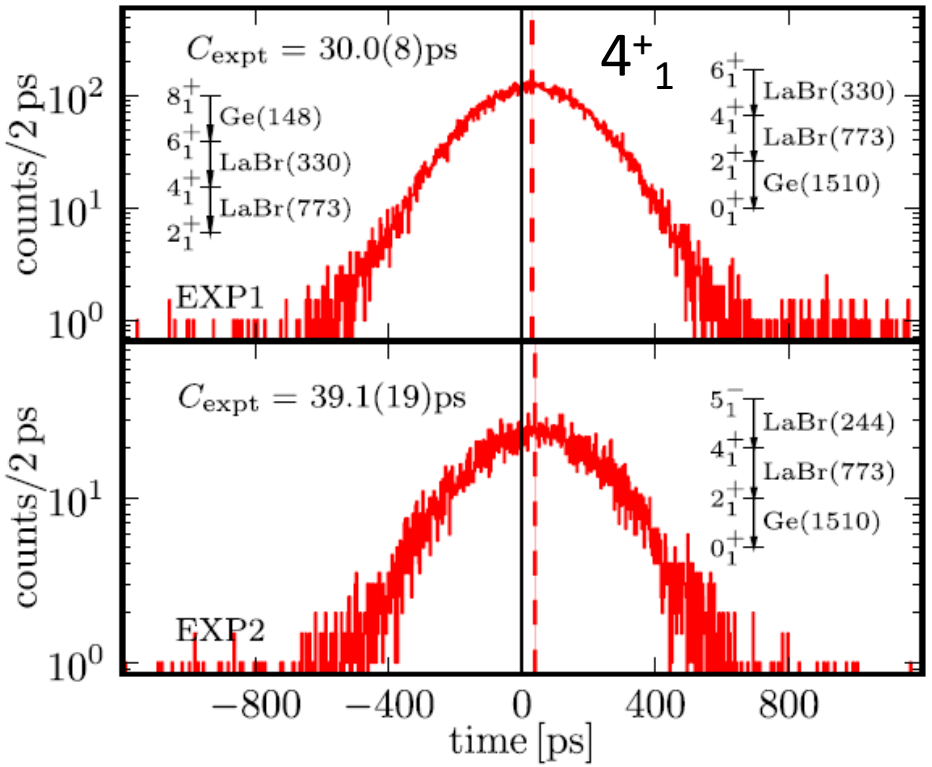

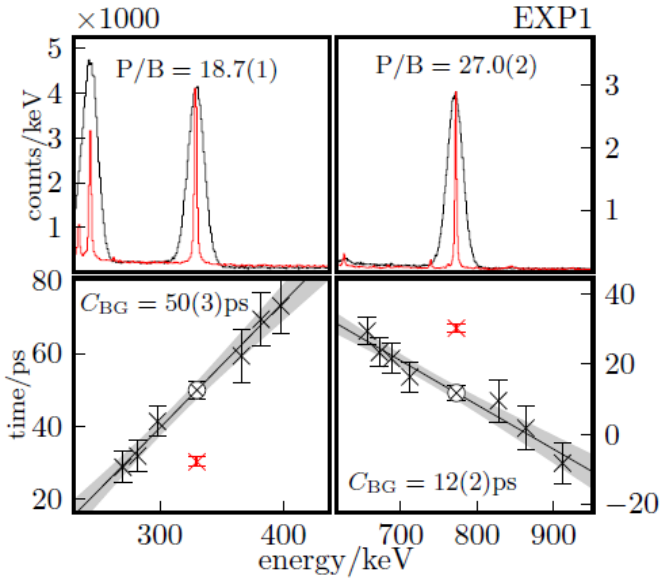

4+1

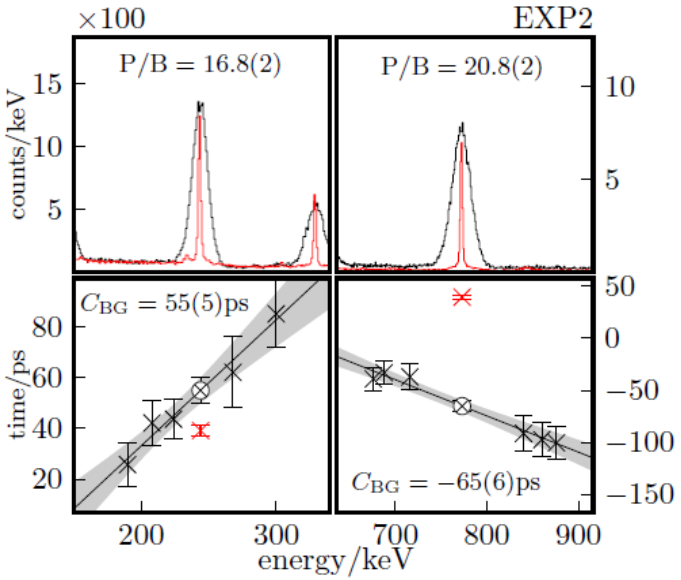

$$C_{PP} = C_{exp} + \tilde{t}_{cor},$$

$$\tilde{t}_{cor} = \frac{P/B(E_f)\,t_{cor}(E_i) + P/B(E_i)\,t_{cor}(E_f)}{P/B(E_i) + P/B(E_f)},$$

$$t_{cor} = \frac{C_{exp} - C_{BG}(E)}{P/B(E)},$$

Exp1: **τ = 22.5(11) ps**

Exp2: τ = 23(2) ps

GANIL: τ = 35.5(6) ps

TABLE I. Summary of the measured mean lifetimes of the states $J_i^{\pi_i}$ and the respective reduced transition probabilities.

$J_i^{\pi_i} \rightarrow J_f^{\pi_f}$	τ_{EXP1} ps	τ_{EXP2} ps	τ_{adopted} ps	Multipolarity	$B(\sigma\lambda; J_i^{\pi_i} \rightarrow J_f^{\pi_f})$ adopted	$B(\sigma\lambda; J_i^{\pi_i} \rightarrow J_f^{\pi_f})$ literature
$2_1^+ \rightarrow 0_1^+$	$\leqslant 3$	$\leqslant 8$	*$\leqslant 3$*	$E2$	$\geqslant 35\ e^2\,\mathrm{fm}^4$	$207(12)\ e^2\,\mathrm{fm}^4$ [30,31]
$4_1^+ \rightarrow 2_1^+$	22.5(11)	23(2)[a]	*22.5(11)*	$E2$	$132^{+7}_{-6}\ e^2\,\mathrm{fm}^4$	$84.3(14)\ e^2\,\mathrm{fm}^4$ [5]
$6_1^+ \rightarrow 4_1^+$	2200(20)	2220(70)	*2200(20)*	$E2$[b]	$81(2)\ e^2\,\mathrm{fm}^4$	$80(3)\ e^2\,\mathrm{fm}^4$ [30,32]
$\rightarrow 5_1^-$				$E1$[b]	$5.3(6) \times 10^{-5}\ e\,\mathrm{fm}^2$	$5.3(7) \times 10^{-5}\ e\,\mathrm{fm}^2$ [30]
$8_1^+ \rightarrow 6_1^+$	$310(3)\times 10^3$[c]	–	*$310(3)\times 10^3$*	$E2$	$28.6(3)\ e^2\,\mathrm{fm}^4$	$32(1)\ e^2\,\mathrm{fm}^4$ [30,33–37]
$5_1^- \rightarrow 4_1^+$	2270(30)	2250(60)	*2270(30)*	$E1$[d]	$\geqslant 1.88(3)\times 10^{-5}\ e\,\mathrm{fm}^2$	$1.91(5)\times 10^{-5}\ e\,\mathrm{fm}^2$ [30,38]
				$M2$[d]	$\leqslant 93\ \mu N^2\,\mathrm{fm}^4$	$\leqslant 98\ \mu N^2\,\mathrm{fm}^4$ [30]
$7_1^- \rightarrow 5_1^-$	$\leqslant 5$	$\leqslant 7$	*$\leqslant 5$*	$E2$	$\geqslant 101\ e^2\,\mathrm{fm}^4$	–
$9_1^- \rightarrow 7_1^-$	37(11)	29(7)	*31(6)*[e]	$E2$	$271^{+65}_{-44}\ e^2\,\mathrm{fm}^4$	–

[a] Averaged value from feeder-decay cascades 244–773 and 330–773 calculated using a Monte Carlo method.
[b] The branching ratio for the 6_1^+ level was derived using the intensities from Ref. [29].
[c] Determined using Ge-LaBr timing.
[d] Mixing ratio $\delta \leqslant 0.05$ from Ref. [39].
[e] Weighted average from EXP1 and EXP2.

5: R. M. Pérez-Vidal et al. Phys. Rev. Let. 129, 112501 (2022)

M. Ley, L. Knafla, J. Jolie, A. Esmaylzadeh, A. Harter, A. Blazhev, C. Fransen, A Pfeil, J.-M. Regis, and P. Van Isacker, PRC108 (2023) 064313.

TABLE II. Experimental and calculated $B(E2)$ values in ^{92}Mo.

				$B(E2; J_i^\pi \to J_f^\pi)$ $(e^2\,\mathrm{fm}^4)$		
υ_i	J_i^π	υ_f	J_f^π	Exp	$\hat{T}_1(E2)$	$\hat{T}_1'(E2)$
2	2_1^+	0	0_1^+	207(12)	89	207(12)
2	4_1^+	2	2_1^+	132^{+7}_{-6}	103	132^{+7}_{-6}
2	6_1^+	2	4_1^+	81(2)	71	81(2)
2	8_1^+	2	6_1^+	28.6(3)	28	28.6(3)

TABLE III. Experimental and calculated $B(E2)$ values in ^{93}Tc.

				$B(E2; J_i^\pi \to J_f^\pi)$ $(e^2\,\mathrm{fm}^4)$		
υ_i	J_i^π	υ_f	J_f^π	Exp	$\hat{T}_1(E2)$	$\hat{T}_1'(E2)$
3	$3/2_1^+$	3	$5/2_1^+$	–	212	256^{+7}_{-6}
3	$3/2_1^+$	3	$7/2_1^+$	–	31	35(1)
3	$5/2_1^+$	3	$7/2_1^+$	–	17	$9.0^{+1.3}_{-1.1}$
3	$5/2_1^+$	1	$9/2_1^+$	–	93	156(6)
3	$7/2_1^+$	1	$9/2_1^+$	–	178	278^{+9}_{-8}
3	$9/2_2^+$	3	$5/2_1^+$	–	23	32(1)
3	$9/2_2^+$	3	$7/2_1^+$	–	20	26(2)
3	$9/2_2^+$	1	$9/2_1^+$	–	11	16.0(5)
3	$9/2_2^+$	3	$11/2_1^+$	–	85	99(1)
3	$9/2_2^+$	3	$13/2_1^+$	–	3.3	4.8(3)
3	$11/2^+$	3	$7/2_1^+$	–	39	63(2)
3	$11/2_1^+$	1	$9/2_1^+$	–	59	87(3)
3	$11/2_1^+$	3	$13/2_1^+$	–	102	132(3)
3	$13/2_1^+$	1	$9/2_1^+$	–	102	166(6)
3	$15/2_1^+$	3	$11/2_1^+$	–	52	62(1)
3	$15/2_1^+$	3	$13/2_1^+$	–	16	$17.7^{+0.4}_{-0.3}$
3	$17/2_1^+$	3	$13/2_1^+$	88(18)[a]	99	114(3)
3	$17/2_1^+$	3	$15/2_1^+$	–	30	30.1(5)
3	$21/2_1^+$	3	$17/2_1^+$	73(5)[b]	57	61(1)

[a]From Ref. [48].
[b]From Ref. [49].

TABLE IV. Experimental and calculated $B(E2)$ values in ^{94}Ru.

				$B(E2; J_i^\pi \to J_f^\pi)$ $(e^2\,\mathrm{fm}^4)$		
υ_i	J_i^π	υ_f	J_f^π	Exp	$\hat{T}_1(E2)$	$\hat{T}_1'(E2)$
4	0_2^+	2	2_1^+	–	30	37(1)
4	0_2^+	4	2_2^+	–	128	164(4)
2	2_1^+	0	0_1^+	165(80)[a]	136	186(4)
4	2_2^+	0	0_1^+	–	7×10^{-6}	$0.07^{+0.06}_{-0.03}$
4	3_1^+	2	2_1^+	–	9×10^{-6}	$0.04^{+0.03}_{-0.02}$
4	3_1^+	4	2_2^+	–	66	79(1)
4	3_1^+	2	4_1^+	–	55	73(2)
4	3_1^+	4	4_2^+	–	12	14(1)
2	4_1^+	2	2_1^+	38(3)[a], 103(24)[b]	12	7.8(7)
2	4_1^+	4	2_2^+	–	25	35(1)
4	4_2^+	2	2_1^+	–	165	224(5)
4	4_2^+	4	2_2^+	–	9.5	15(1)
4	5_1^+	4	3_1^+	–	16	22(1)
4	5_1^+	2	4_1^+	–	124	173(4)
4	5_1^+	4	4_2^+	–	8.3	$5.4^{+0.4}_{-0.3}$
4	5_1^+	2	6_1^+	–	26	38(1)
4	5_1^+	4	6_2^+	–	16	23(1)
2	6_1^+	2	4_1^+	3.0(2)[b]	8.0	$3.9^{+0.5}_{-0.4}$
2	6_1^+	4	4_2^+	–	60	80(2)
4	6_2^+	2	4_1^+	–	25	36(1)
4	6_2^+	4	4_2^+	–	107	130^{+3}_{-2}
2	8_1^+	2	6_1^+	0.09(1)[b]	3.2	1.0(2)
2	8_1^+	4	6_2^+	–	98	137(3)
4	8_2^+	2	6_1^+	–	61	82(2)
4	8_2^+	4	6_2^+	–	21	27(1)
4	10_1^+	2	8_1^+	–	105	147(3)
4	10_1^+	4	8_2^+	–	22	23.3(4)

[a]From Ref. [5].
[b]From Ref. [13].

The effective charge in the one-body operator $\mathbf{T}_1$(E2) is obtained from the quadrupole moment of the $9/2^+$ ground state of ^{91}Nb, with the experimental value and uncertainty $Q(9/2^+) = -25(3)$ e fm2.

The operator $\mathbf{T'}_1$(E2) has effective charges that depend on the two-nucleon states $(\pi 1g_{9/2})^2$ and which will be used to predict transition rates in $(\pi 1g_{9/2})^n$ states with $n>2$.

a: R. M. Pérez-Vidal et al. Phys. Rev. Let. 129, 112501 (2022)

τ_{4^+} = 87(8) ps from plunger measurement at GANIL

b: B. Das et al. Phys. Rev. C 105, L031304 (2022)

τ_{4^+} =32(11) ps from fast timing measurement at GSI

^{93}Tc:

Very few absolute transition rates are known in this three valence proton nucleus:

the B(E2; $17/2_1^+ \rightarrow 13/2_1^+$)= 88(18) e^2fm^4 and the B(E2; $21/2_1^+ \rightarrow 17/2_1^+$)*= 66(2) e^2fm^4

A fast timing experiment was performed in Cologne using the ^{90}Zr(^{6}Li, 3n)^{93}Tc @ 31MeV reaction on a : 5.3mg/cm² ^{90}Zr (98% enriched) target.

Results:

state J^π	E_{state} keV	cascade keV−keV	Ge gate keV	$^P/_B$ feeder−decay	τ_{expt} ps	$\tau_{adopted}$ ps	$\tau_{literature}$ ps
$(^{11}/_2)_1^+$	1516	629−1516	—	2.17(2)−3.45(2)	2(2)	*≤4*	—
$(^{13}/_2)_1^+$	1434	750−1434	350 —	15.0(4)−12.8(3) 6.38(4)−6.85(4)	2(4) 0(1)	*≤6*	$< 14 \times 10^3$ [29]
$(^{17}/_2)_1^+$	2185	350−750	1434 —	13.0(3)−13(2) 5.20(2)−4.33(2)	30(4) 28(1)	*28(1)*	39(7)[30]
$(^{21}/_2)_1^+$	2535	1722−350	750, 1434 [b]	1.31(4)−4.1(1)	2310(90) [c]	*2310(90)*	2320(80) [a] [31–33]

transition $J_i^{\pi_i} \rightarrow J_f^{\pi_f}$	E_γ keV	$\sigma\lambda$	$B(\sigma\lambda; J_i^{\pi_i} \rightarrow J_f^{\pi_f})$ adopted	$B(\sigma\lambda; J_i^{\pi_i} \rightarrow J_f^{\pi_f})$ literature	$B(E2)$ single-j [9] $\hat{T}_1(E2) \mid \hat{T}_1'(E2)$	shell model $B(E2)$ SR88MHJM
$(^{11}/_2)_1^+ \rightarrow (^7/_2^+)_1$	836	(E2)	≥ 19	—	39 | 63(2)	39
$(^{11}/_2)_1^+ \rightarrow {}^9/_2^+_1$	1516	M1+E2	≥ 24 [d]	—	59 | 87(3)	78
$(^{13}/_2)_1^+ \rightarrow {}^9/_2^+_1$	1434	E2	≥ 22	≥ 0.009 [36]	102 | 166(6)	140
$(^{17}/_2)_1^+ \rightarrow (^{13}/_2)_1^+$	750	E2	122(5)	88(18) [30]	99 | 114(3)	99
$(^{21}/_2)_1^+ \rightarrow (^{17}/_2)_1^+$	350	E2	66(3)	66(2) [e]	57 | 61(1)	57

* Nuclear Data Sheets Update for A = 93 after correction for (21/2)+

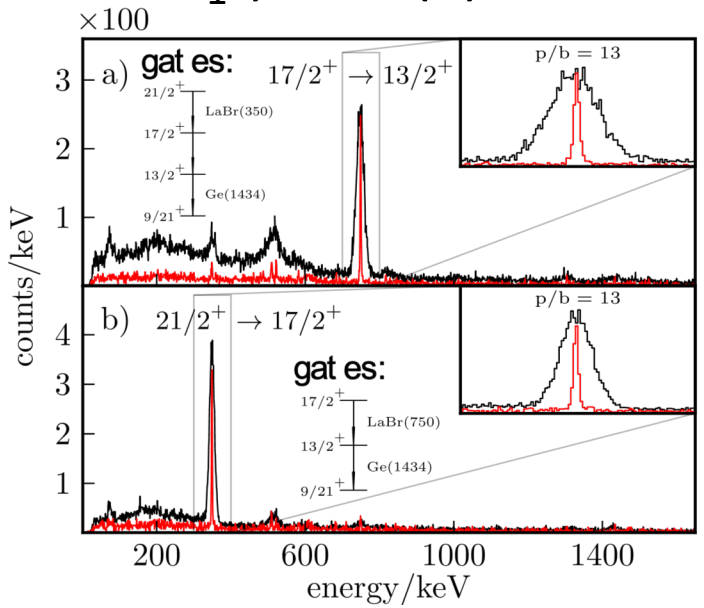

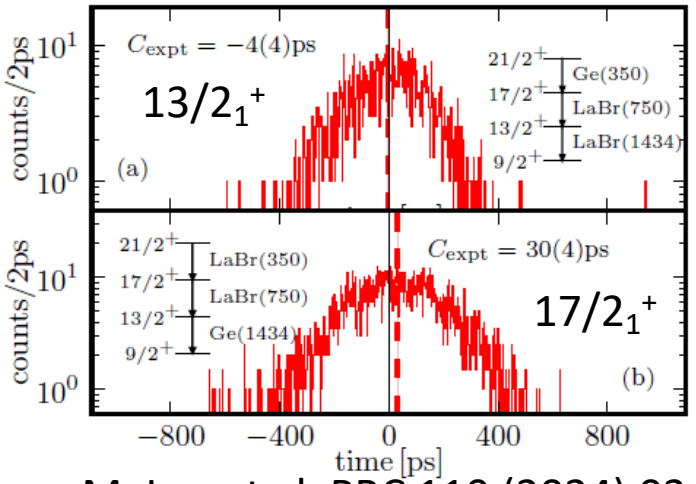

M. Ley et al. PRC 110 (2024) 034320

^{94}Ru:

Fast Timing experiment at Cologne Tandem

^{92}Mo(^{4}He, 2n)^{94}Ru @ 28MeV on 5.5mg/cm²

^{92}Mo (98% enriched)

Results:

state J^π	E_{state} keV	cascade keV−keV	Ge gate keV	P/B feeder−decay	τ_{expt} ps	$\tau_{adopted}$ ps	$\tau_{literature}$ ps
2_1^+	1431	756−1431	311	60.1(2)−67.2(2)	≤2	*≤2*	0.8(4) [10]
4_1^+	2187	311−756 438−756	1431	24.2(2)−41.8(4) 10.3(3)−10.4(2)	66(2) 65(4)	*66(2)* [a]	32(11) [8] 87(8) [10]
6_1^+	2498	146−311	756, 1431 [b]	5.58(3)−7.24(4)	95.5(6)×10^3 [c]	*95.5(6)×10^3*	94(3)×10^3 [18]
10_1^+	3991	498−1347	1079	12(1)−11(1)	≤13 [d]	*≤13*	<5 [28]
5_1^-	2624	1033−438 1033−126	756, 1431 [b] 311, 756, 1431 [b]	2.05(5)−3.05(7) 2.32(5)−1.96(4)	1170(40) [c] 1300(40) [c]	*1240(30)* [a]	731(67) [28]
7_1^-	3658	540−1033	438, 756, 1431 [b]	5.2(2)−5.7(2)	≤5	*≤5*	—
9_1^-	4197	292−540	438, 1033 [b]	2.42(7)−3.42(9)	139(8)	*139(8)*	—
11_1^-	4489	1079−498	1347	4.5(4)−2.9(2)	900(100) [c]	*900(100)*	1097(50) [28]

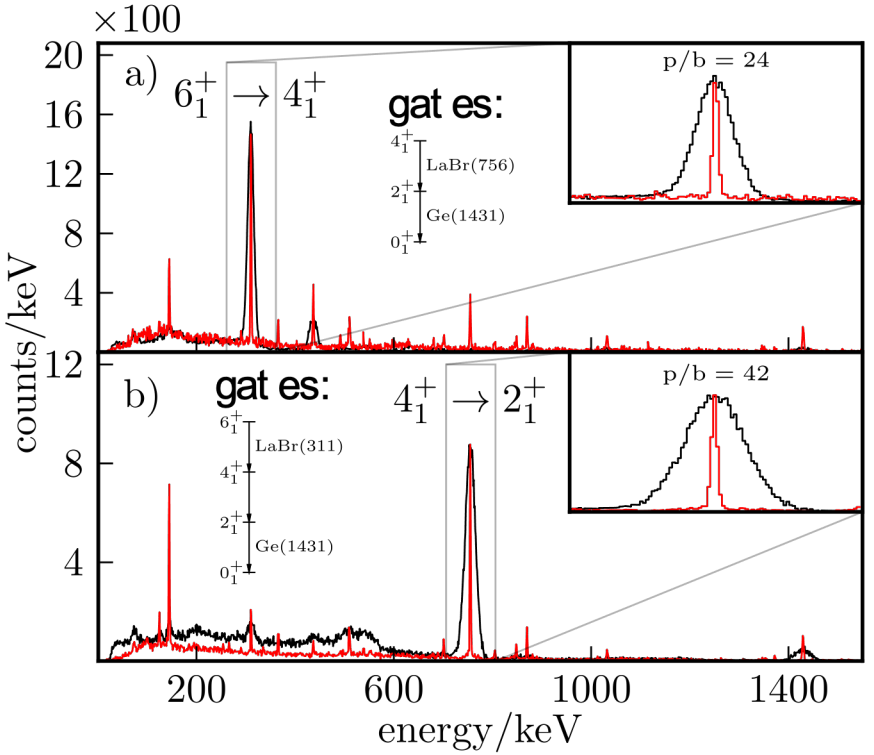

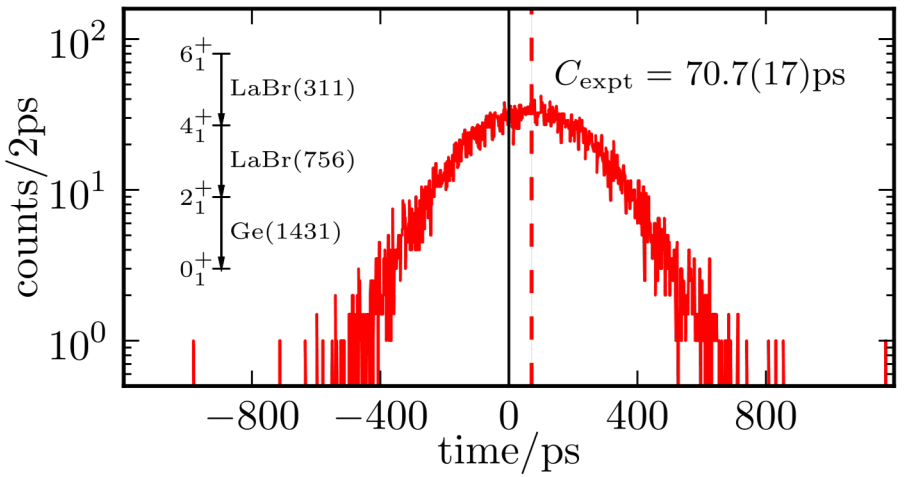

M. Ley, J. Jolie, L. Knafla, A. Blazhev, A. Esmaylzadeh, C. Fransen, A Pfeil, J.-M. Regis, and P. Van Isacker, Phys.Rev C 110 (2024) 034320.

transition $J_i^{\pi_i} \to J_f^{\pi_f}$	E_γ keV	$\sigma\lambda$	$B(\sigma\lambda; J_i^{\pi_i} \to J_f^{\pi_f})$ adopted	$B(\sigma\lambda; J_i^{\pi_i} \to J_f^{\pi_f})$ literature	$B(E2)$ single-j [9] $\hat{T}_1(E2) \mid \hat{T}'_1(E2)$	shell model $B(E2)$ SR88MHJM
$2_1^+ \to 0_1^+$	1431	(E2)	≥ 68	165(80) [10]	136 | 186(4)	177
$4_1^+ \to 2_1^+$	756	(E2)	50(2)	38(3), 103(24) [10], [8]	12 | 7.8(7)	7.4
$6_1^+ \to 4_1^+$	311	E2	2.85(2)	3.0(2) [8]	8.0 | $3.9^{+0.5}_{-0.4}$	4.6
$8_1^+ \to 6_1^+$	146	E2	—	0.09(1) [38, 39]	3.2 | 1.0(2)	1.5
$(10)_1^+ \to 8_1^+$	1347	E2	≥ 14	≥ 37 [a]	105 | 147(3)	134
$5_1^- \to 6_1^+$	126	E1	$7.7(3) \times 10^{-5}$	$13.3(15) \times 10^{-5}$ [18]	—	—
$5_1^- \to 4_1^+$	438	E1	$4.05(12) \times 10^{-6}$	$6.9(8) \times 10^{-6}$ [18]	—	—
$(7^-)_1 \to 5_1^-$	1033	(E2)	≥ 139 [b]	—	—	178
$(9)_1^- \to (8^+)_2$	267	(E1)	$2.4(2) \times 10^{-5}$ [c]	—	—	—
$(9)_1^- \to (7^-)_1$	540	(E2)	98(6) [b]	—	—	7×10^{-8}
$(9)_1^- \to 8_1^+$	1553	(E1)	$1.5(1) \times 10^{-7}$ [c]	—	—	—
$(11)_1^- \to (9)_2^-$	151	E2	128^{+25}_{-22}	107(18) [18]	—	182
$(11)_1^- \to (9)_1^-$	292	E2	134^{+17}_{-13}	111(5) [18]	—	6×10^{-8}
$(11)_1^- \to (10)_1^+$	498	E1	$3.8(5) \times 10^{-6}$	$3.1(3) \times 10^{-6}$ [18]	—	—

Also here the main problem is the lifetime of the first 4^+ state. Two recent RIB experiments at FAIR Phase 0 and GANIL yielded contradictory results: $\tau = 32(11)$ps [1] and $\tau = 87(8)$ps [2]. We got $\tau = 66(2)$ps or B(E2; $4^+ \rightarrow 2^+$)= 50(2) e^2fm^4 while the single-j prediction is B(E2; $4^+ \rightarrow 2^+$)= 7.8(7) e^2fm^4.

To obtain an understanding of this disagreement, it is essential to consider that for four particles or four holes in a $j = 9/2$ orbit two 4^+ levels with v = 2 and v = 4 occur close in energy. Given that the $\Delta v = 2$ transition is ~14 times faster than the one with $\Delta v = 0$, a small admixture of v = 4 in the first 4^+ state can considerably alter the B(E2; $4^+ \rightarrow 2^+$) value.

However, the v = 4 4^+ state is solvable for *any* interaction in a $j = 9/2$ orbital, which means that in order to mix with the v = 2 state necessarily must involve components outside the $0g9/2$ space.

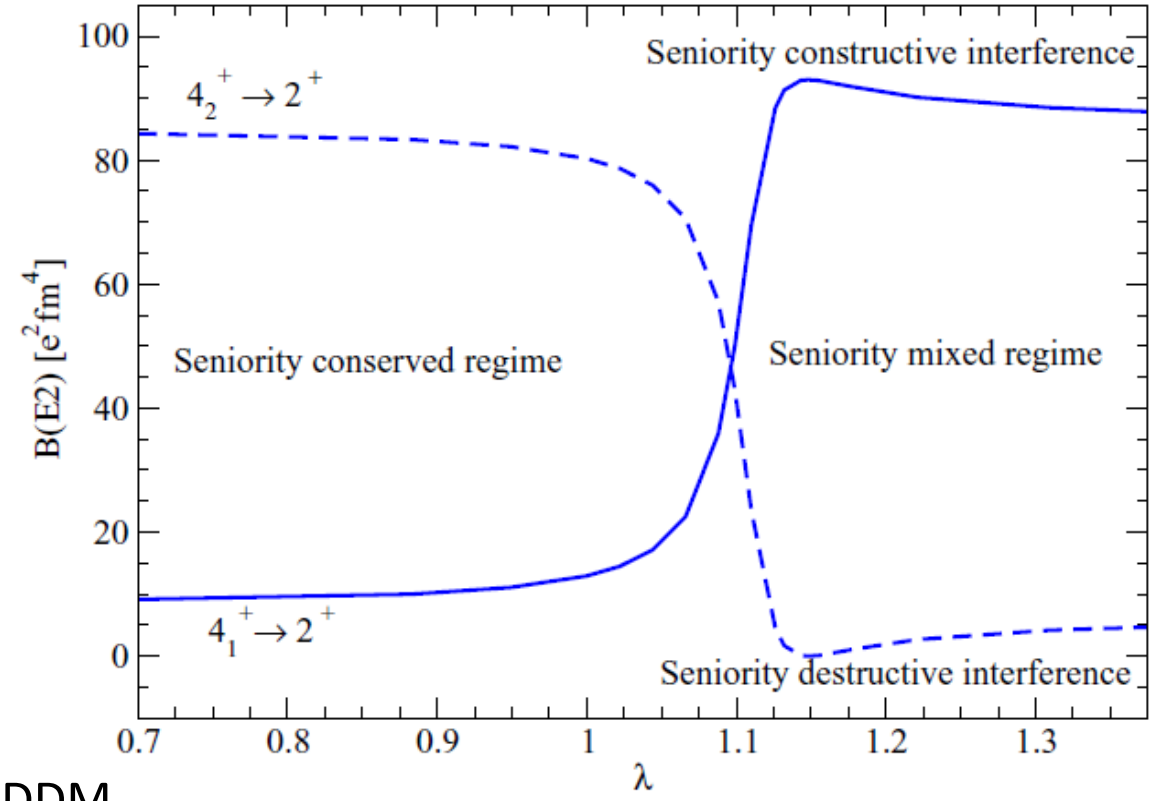

[1] B. Das et al. Phys. Rev. C 105, L031304 (2022) Fast Timing

[2] R. M. Pérez-Vidal et al. Phys. Rev. Let. 129, 112501 (2022) RDDM

Assuming an ad hoc mixed structure of the first 4^+ and 6^+ state:

$$|4_1^+\rangle = \alpha_4|4^+_{v=2}\rangle + \beta_4|4^+_{v=4}\rangle,$$
$$|6_1^+\rangle = \alpha_6|6^+_{v=2}\rangle + \beta_6|6^+_{v=4}\rangle,$$

transition	ξ_1	ξ_2	expt. $B(E2)$	SM $B(E2)$ [5]
$4_1^+ \to 2_1^+$	21^{+3}_{-7}	86^{+15}_{-5}	50(2)	85.2
$6_1^+ \to 4_1^+$	$2.8^{+2.1}_{-1.7}$	$2.8^{+3.1}_{-1.9}$	2.85(2)	17.3
$8_1^+ \to 6_1^+$	$0.11^{+0.14}_{-0.11}$	$0.12^{+0.17}_{-0.12}$	0.09(1)	0.77

Two almost equally good solutions ξ_1 and ξ_2 are obtained.

The values are compared to a large scale shell model calculation using a 1g,2d,3s configuration with up to 4p-4h excitations across Z = 50 [5].

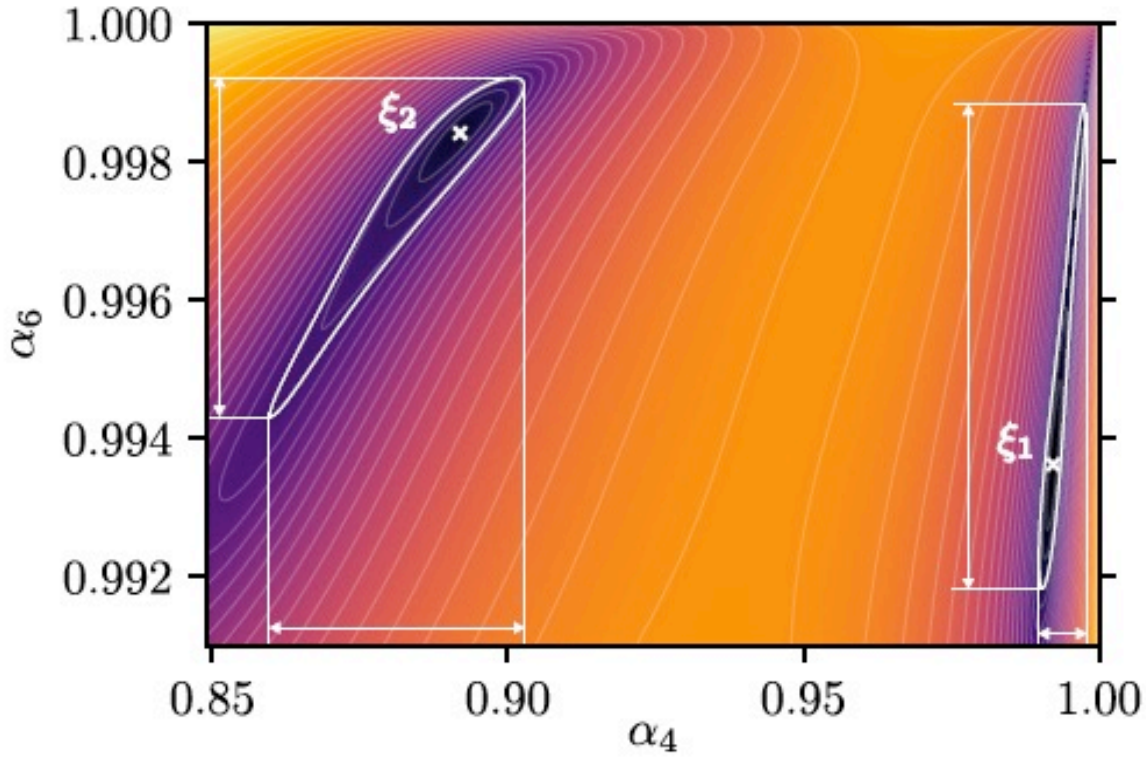

[5] H. Mach *et al.*, Phys. Rev. C **95**, 014313 (2017).

4. Conclusions and outlook

Excellent agreement with the single-j predictions for the B(E2) values in ^{211}At was obtained when using the B(E2) values in ^{210}Po as input.

In order to perform the same for the N= 50 isotones, precise lifetimes in ^{92}Mo were determined to serve as input for the calculations with more than two protons.

A fast timing experiment in ^{93}Tc yields promising results but more B(E2) values are needed, especially for low spin states.

The B(E2; $4^+ \rightarrow 2^+$) in ^{94}Ru was measured to solve contradictory results from RIB experiments, but it still disagrees with the single-j predictions and LSSM calculations.

Much more stable and RIB experiments are needed.